Size effect on the magnetic phase in $Sr_4Ru_3O_{10}$

2016 New J. Phys. 18 053019

(http://iopscience.iop.org/1367-2630/18/5/053019)

New Journal of Physics
The open access journal at the forefront of physics

Deutsche Physikalische Gesellschaft DPG
IOP Institute of Physics

Published in partnership with: Deutsche Physikalische Gesellschaft and the Institute of Physics

OPEN ACCESS

RECEIVED
10 December 2015

REVISED
15 March 2016

ACCEPTED FOR PUBLICATION
26 April 2016

PUBLISHED
12 May 2016

PAPER

Size effect on the magnetic phase in $Sr_4Ru_3O_{10}$

Yan Liu[1,2], Jiyong Yang[1,3], Weike Wang[1], Haifeng Du[1,3], Wei Ning[1,3], Langsheng Ling[1,3], Wei Tong[1,3], Zhe Qu[1,3], Zhaorong Yang[1,3,4], Mingliang Tian[1,3,4], Gang Cao[5] and Yuheng Zhang[1,2,4]

[1] High Magnetic Field Laboratory, Chinese Academy of Sciences, Hefei 230031, Anhui, People's Republic of China
[2] University of Science and Technology of China, Hefei 230031, Anhui, People's Republic of China
[3] Hefei Science Center, Chinese Academy of Sciences, Hefei 230031, Anhui, People's Republic of China
[4] Collaborative Innovation Center of Advanced Microstructures, Nanjing University, Nanjing 210093, People's Republic of China
[5] Center for Advanced Materials, Department of Physics and Astronomy, University of Kentucky, Lexington, Kentucky 40506, USA

E-mail: jyyang@hmfl.ac.cn **and** tianml@hmfl.ac.cn

Keywords: $Sr_4Ru_3O_{10}$, metamagnetic transition, size effect, Hall effect

Abstract

High quality $Sr_4Ru_3O_{10}$ nanoflakes are obtained by the scotch tape-based micro-mechanical exfoliation method. The metamagnetic transition temperature T_m^{flake} is found to decrease in line with the decrease of thickness, while the ferromagnetic (FM) phase, the ordinary, and anomalous Hall effects (OHE and AHE) are independent on the thickness of the flake. Analysis of the data demonstrates that the AHE reflects the FM nature of $Sr_4Ru_3O_{10}$, and the decrease of thickness favors the Ru moments aligned in the *ab*-plane, which induces a decrease of the metamagnetic transition temperature compared with the bulk.

1. Introduction

Ruthenium oxide perovskites $Sr_{n+1}Ru_nO_{3n+1}$ ($n = 1, 2, 3, \infty$) are strongly correlated materials involving complex interactions between the charge, spin, orbit and lattice degrees of freedom. Their ground states present a rich of exotic physical properties, such as the unconventional spin-triplet superconductivity in Sr_2RuO_4 ($n = 1$) [1], the quantum criticality and nematicity in $Sr_3Ru_2O_7$ ($n = 2$) [2–4], and the spontaneous itinerant ferromagnetism in the infinite layer of $SrRuO_3$ ($n = \infty$) [5, 6]. $Sr_4Ru_3O_{10}$ is the $n = 3$ member of the $Sr_{n+1}Ru_nO_{3n+1}$ family. It belongs to quasi-two-dimensional metal with an orthorhombic unit cell, which is composed of triple layers of corner-shared RuO_6 octahedra separated by double rock-salt Sr-O layer [7]. This member has attracted considerable attention in recent years due to its unique magnetic properties [7–17]. By applying a magnetic field H (0.01T) along the *c*-axis, the temperature dependent magnetization $M_c(T)$ exhibits a FM transition at a Curie temperature $T_c \sim 105$ K, followed by another sharp transition at temperature T_m^{bulk} of about ~50 K with a large irreversibility. In contrast, by applying a field ($H = 0.01$ T) within the *ab*-plane, the $M_{ab}(T)$ displays a weak cusp at T_c and a pronounced peak at T_m^{bulk} with a much smaller irreversibility, and below about 20 K, the M_{ab} is almost unmeasurable [7, 8]. Interestingly, if the in-plane field reaches a critical field H_c, a rapid increase of M_{ab} in a narrow range of magnetic field is observed on the *M*-*H* curves at temperatures below T_m^{bulk}, and the H_c increases with the decrease of temperature ($H_c^{2K} \sim 2$ T) [8]. This transition is considered to be the metamagnetic transition.

The metamagnetic transition observed in $Sr_4Ru_3O_{10}$ below T_m^{bulk} contains rich physics associated with the lattice, spin, orbit, and electronic inhomogeneity, which has not been well understood. Firstly, this transition is accompanied by strong spin-lattice coupling [9, 14, 18]. The crystal structure undergoes a significant change when the applied in-plane field crosses over the critical field H_c [9, 14]. Secondly, the occurrence of the transition is possibly through a phase separation process with magnetic domain formation, for the in-plane magnetoresistivity near H_c exhibits large hysteresis or multiple ultra-sharp steps at extreme low temperatures (<1 K) [10, 11, 17]. Thirdly, the angle-resolved magnetization and magnetoresistivity suggest the metamagnetic transition is orbit-dependent, where the Ru $4d_{xz,yz}$ orbit is responsible for the metamagnetic transition while the $4d_{xy}$ orbit is ferromagnetic in the ground state [12, 13]. The understanding of the metamagnetic transition in

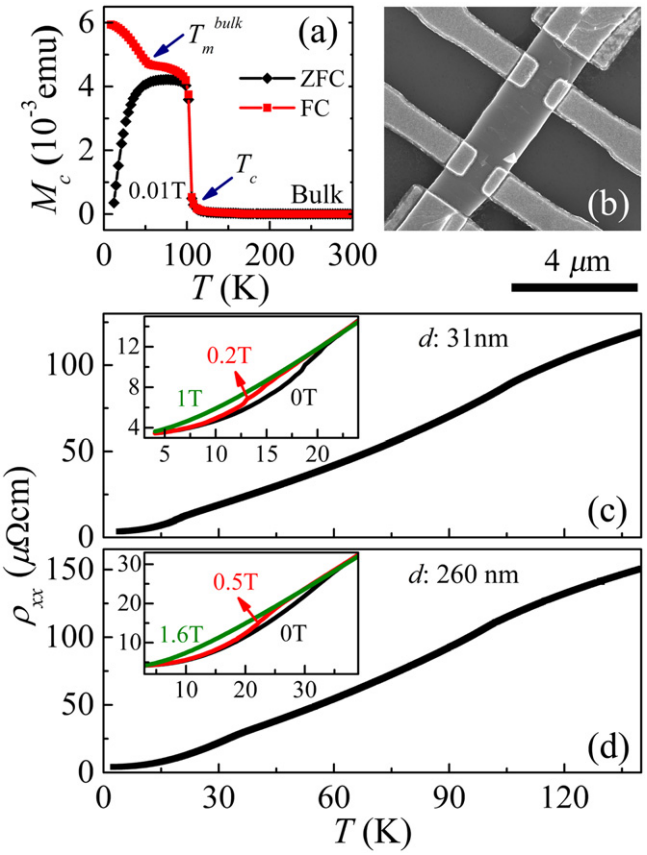

Figure 1. (a) Magnetization as a function of temperature measured along the *c*-axis at 0.01 T of the $Sr_4Ru_3O_{10}$ single crystal under zero-/or field cooling condition. (b) SEM image of a $Sr_4Ru_3O_{10}$ flake ($d = 260$ nm) with patterned electrodes. (c) and (d) are, respectively, the temperature dependence of the longitudinal resistivity ρ_{xx} of the $Sr_4Ru_3O_{10}$ flakes with different thickness *d*; the insets are, respectively, the blow-up of the ρ_{xx}-*T* curves in low-*T* range measured under in-plane fields.

$Sr_4Ru_3O_{10}$ is challenged by recent neutron study, where the Ru moments at zero field and below T_c are found to be FM-aligned along the *c*-axis only, there is no any signature of either long-range antiferromagnetic (AFM) or FM order in the *ab*-plane [14]. However, the neutron data cannot exclude a possibility that the metamagnetism is a field-induced short-range AFM order to FM transition. To date, the magnetic nature of $Sr_4Ru_3O_{10}$ below T_m^{bulk} is still unclear and remains elusive.

In this work, we present the electrical transport measurements of two mechanically exfoliated $Sr_4Ru_3O_{10}$ nanoflakes with thickness of 31 nm and 260 nm. It finds that the metamagnetic transition temperature, T_m^{flake}, in the flake is much smaller than the bulk, $T_m^{bulk} \sim 50$ K, and decreases with decreasing thickness, but its saturation field H_s along the *c*-axis increases with the decrease of thickness, indicating the Ru moment in the thinner sample is more difficult to be aligned along the *c*-direction. However, the FM transition, the ordinary and anomalous Hall effects are independent on the thickness, where the dominant carriers derived from the ordinary Hall coefficient R_0 are always hole-type and the anomalous Hall conductivity σ_{xy}^A follows the typical scaling law $\sigma_{xy}^A \propto \sigma_{xx}^{\varphi}$ (σ_{xx}: longitudinal conductivity) with different scaling exponent, $\varphi \sim 1$, 0 and 1.6, as the increase of temperature *T*. The decrease of the metamagnetic transition temperature thus cannot be attributed to the changes of the unit cell or the electronic structures, but can be understood by the shape anisotropy induced rearrangement of the Ru moments due to the size effect.

2. Experimental

$Sr_4Ru_3O_{10}$ single crystal is grown by the flux technique [8]. The temperature dependent magnetization of the bulk crystal along the *c*-axis measured under 0.01 T is shown in figure 1(a), which is well consistent with those reported previously [7, 8]. The characteristic temperatures $T_m^{bulk} \sim 50$ K and $T_c \sim 105$ K of the single crystal are indicated by the arrows. The $Sr_4Ru_3O_{10}$ flakes are obtained by the scotch tape-based micro-mechanical exfoliation from the bulk single crystal, and then transferred to a silicon substrate covered with 300 nm-thick silicon dioxide on the top of the surface. The thickness, *d*, of the flake is determined by atomic force microscopy. Conventional six terminal electrical contacts are made using electron-beam lithography (EBL) technique. To

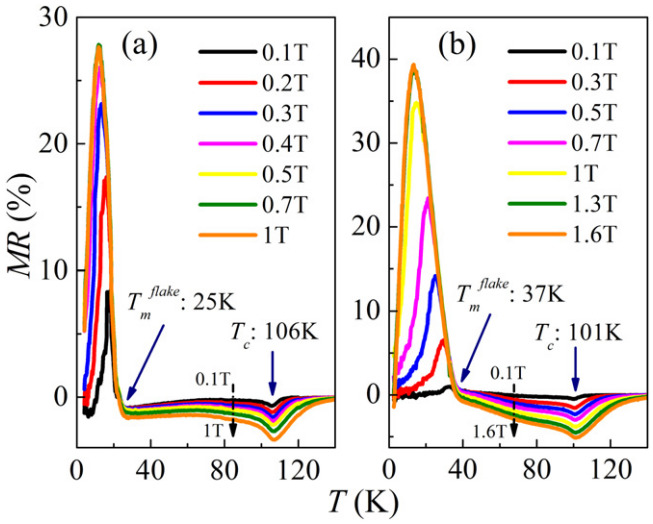

Figure 2. The magnetoresistivity *MR* of $Sr_4Ru_3O_{10}$ flakes as a function of temperature *T* under various in-plane magnetic fields. (a) $d = 31$ nm; (b) $d = 260$ nm.

ensure ohmic contacts, we etch the e-beam patterned contact areas for a few seconds by *in situ* Ar-plasma to remove the possible residual PMMA resist firstly, and then deposit 5 nm Ti and 150 nm Au working as the electrical leads by thermal evaporation. With this process, the successful rate for ohmic contacts is higher than 90%, and the resistance ratio between the contact resistance and the sample is usually less than 15%. The scanning electron microscope (SEM) image of a device with patterned electrode is shown in figure 1(b). The longitudinal resistivity (ρ_{xx}) and the Hall resistivity (ρ_{xy}) are measured as functions of temperature (T) and external magnetic field (H) by a physical property measurement system (PPMS, Quantum Design). The ρ_{xx} is measured by the standard four-probe configuration, where the contact resistance is believed to be negligible. The Hall resistance ρ_{xy} is determined from $\rho_{xy} = [\rho_{xy}(H)\text{-}\rho_{xy}(\text{-}H)]/2$ in order to subtract the longitudinal component of ρ_{xx} arising from the small misalignment of the transverse contacts.

3. Results and discussion

Figures 1(c) and (d) show ρ_{xx} versus T curves of two flakes ($d = 31$ and 260 nm) measured at zero magnetic field. For each flake, the ρ_{xx} decreases monotonically as T decreases. The residual resistance ratio, $RRR = \rho_{xx}{}^{300\text{ K}}/\rho_{xx}{}^{2\text{ K}}$, of each flake reaches about 60 (data not shown), indicating the crystals are high quality, where the residual resistivity of both flakes at 2 K is about 3.77 $\mu\Omega$.cm ($d = 31$ nm) or 4.15 $\mu\Omega$.cm ($d = 260$ nm). Two anomalies on the resistivity can be clearly identified from the magnetoresistivity (*MR*) measured under various in-plane magnetic fields H as shown in figure 2, where *MR* is defined as $[\rho_{xx}(H)\text{-}\rho_{xx}(0)]/\rho_{xx}(0)$. The data is obtained by the zero field cooling from above 160 K to exclude the influence of the field history. The 'valley' observed on the *MR*-*T* curves is as expected due to the itinerant FM nature of $Sr_4Ru_3O_{10}$ [8], which is caused by the suppression of carrier scattering from spin fluctuations under in-plane magnetic field [19]. The T_c is determined to be ~106 K and 101 K for the 31 nm- and 260 nm-thick flakes, respectively, from the negative maximum of the 'valley' [19], which is almost independent on the thickness and consistent with the bulk. With decreasing T below T_c, the $Sr_4Ru_3O_{10}$ undergoes another transition called the metamagnetic transition at about $T_m^{flake} \sim 25$ K and 37 K for the 31 nm- and 260 nm-thick flakes, below T_m^{flake} the *MR* shows a positive behavior, while above which the *MR* is always negative due to the FM nature of $Sr_4Ru_3O_{10}$. This feature is consistent with that reported in the bulk [11], except for the T_m^{flake} is almost 20 K lower than the $T_m^{bulk} \sim 50$ K. It finds that the metamagnetic transition temperature decreases with decreasing the thickness of the flake, while the T_c remains unchanged. Previously, both the electronic and lattice structures have been suggested to be the driving force for the formation of the metamagnetic phase [7, 12–15]. A fact that our sample preparation process does not make any variations of the electronic or lattice structures provides an indication that the metamagnetic transition in $Sr_4Ru_3O_{10}$ should have an origin of internal magnetic orders, which maybe changed as the decrease of thickness. To understand the mechanism in detail, we performed the Hall effect study on the flakes.

Figure 3 shows the H-dependence of ρ_{xy} at various temperatures, where H is applied perpendicular to the *ab*-plane of the flake. As a FM nature of $Sr_4Ru_3O_{10}$ below T_c, both the OHE and AHE make contributions to the total Hall resistivity [20], characterized by the 'knee' profile as shown in figure 3. At temperatures far above T_c, the

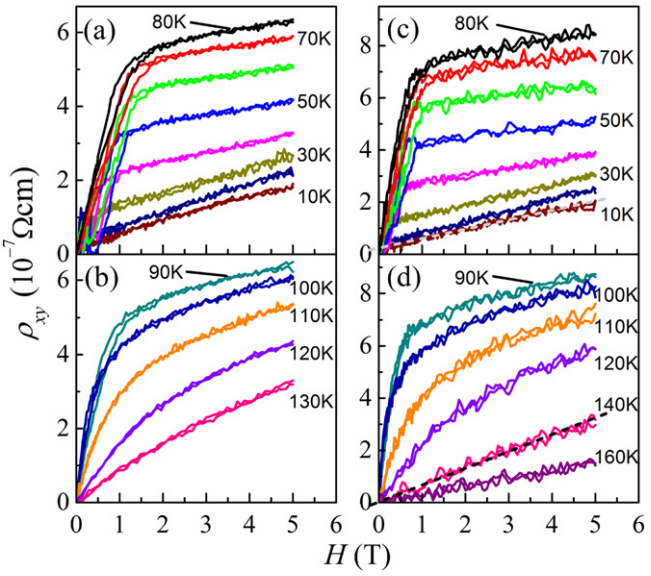

Figure 3. Hall resistivity ρ_{xy} of the $Sr_4Ru_3O_{10}$ flakes as a function of magnetic field H along the c-axis at various temperatures. (a), (b) are for $d = 31$ nm; (c), (d) for $d = 260$ nm.

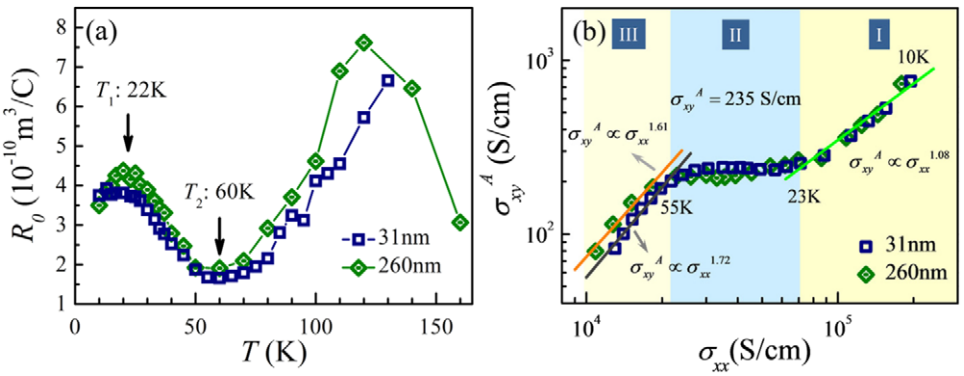

Figure 4. (a) The temperature dependence of the ordinary Hall coefficient R_0. (b) The scaling relation between the anomalous Hall conductivity $\sigma_{xy}{}^A$ and the longitudinal conductivity σ_{xx}.

OHE resistivity $\rho_{xy}{}^o$ governs the total ρ_{xy} with a linear H dependence of $\rho_{xy}{}^o = R_0 H$ (e.g. see the dashed line in figure 3(d)), which is due to the orbital effect of H on the carriers, here R_0 is the ordinary Hall coefficient. With decreasing T, the AHE gradually dominates the ρ_{xy}, and the AHE resistivity $\rho_{xy}{}^A$ reaches a maximum at about 80 K. Then $\rho_{xy}{}^A$ decreases rapidly with the further decrease of T and becomes extremely small at 10 K but can still be recognized (e.g. see the dashed line in figure 3(c)). In spite of the FM-induced hysteresis behavior in the low field range, the trace of the observed ρ_{xy} at a fixed temperature can be well described by the equation of $\rho_{xy} = R_0 H + \rho_{xy}{}^A$, which contains both the OHE and AHE components. The ordinary Hall coefficient R_0 can be extracted from the high field slope, *i.e.* $d\rho_{xy}/dH$ for $H = 5$ T, of the Hall isotherm, and the $\rho_{xy}{}^A$ below T_c can be simultaneously obtained by extrapolating the linear term to the zero field.

The ordinary Hall coefficient R_0 as a function of temperature is shown in figure 4(a). R_0 is positive in the whole temperature range, indicating the dominant carriers in $Sr_4Ru_3O_{10}$ are holes. The R_0-T curves for both flakes present almost a same '*S*-shaped'-like behavior. Specifically, the $R_0(T)$ shows a maximum near $T_1 \sim 22$ K and a minimum near $T_2 \sim 60$ K below T_c, and these kinks show no direct correlation with the magnetic structures, such as the metamagnetic transition near $T_m{}^{flake}$ and the FM transition at T_c. Generally, the temperature dependent $R_0(T)$ in quasi-two-dimensional metal is related to the changes of the wave vector dependent electron mean free path or the reconstruction of the Fermi surface [21, 22]. The almost identical $R_0(T)$ in both flakes implies that the electronic structures are almost independent on the thickness of the flakes as expected. We noticed that both $R_0(T)$ display a similar T-dependent feature as the variations of the lattice

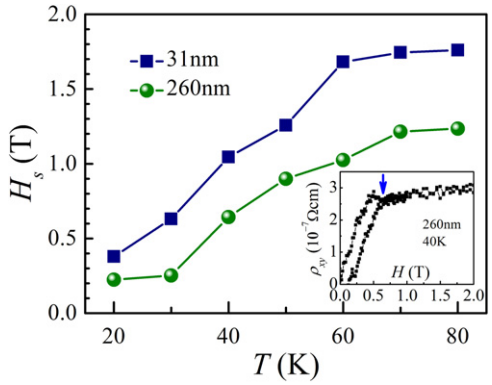

Figure 5. The saturation magnetic field H_s of the two $Sr_4Ru_3O_{10}$ flakes as a function of temperature. The inset show a typical ρ_{xy}-H curve of the 260-thick flake measured at 40 K under magnetic fields along the c-axis.

parameter c determined by the neutron diffraction study [14], indicating that the variations of R_0 in $Sr_4Ru_3O_{10}$ might be closely connected to this structural change.

Now we turn to the AHE component and use the universal scaling relation [20], ${\sigma_{xy}}^A \propto {\sigma_{xx}}^\varphi$, to uncover the physical implication below T_c (~100 K) in the flakes, where ${\sigma_{xy}}^A$ and σ_{xx} are, respectively, the anomalous Hall and longitudinal conductivity, and φ is the scaling exponent. Here, ${\sigma_{xy}}^A$ is estimated by ${\sigma_{xy}}^A = {\rho_{xy}}^A/[{\rho_{xx}}^2 + ({\rho_{xy}}^A)^2] \approx {\rho_{xy}}^A/{\rho_{xx}}^2$ since ${\rho_{xy}}^A$ is at least two orders smaller than ρ_{xx} in our case. As shown in figure 4(b), the ${\sigma_{xy}}^A$ is also independent on the thickness of the flake, and can be categorized into three regions labeled as I, II and III with an exponent of $\varphi \sim 1.08$ in $T < 23$ K (or $\sigma_{xx} > 7.5 \times 10^4$ S cm^{-1}), $\varphi \sim 0$ with ${\sigma_{xy}}^A = 235$ S cm^{-1} in 23 K $< T <$ 55 K (or 2.2×10^4 S cm^{-1} $< \sigma_{xx} < 7.5 \times 10^4$ S cm^{-1}) and $\varphi \sim 1.61$ or 1.72 in $T >$ 55 K (or $\sigma_{xx} < 2.2 \times 10^4$ S cm^{-1}), respectively. It is well-known that both the extrinsic and intrinsic mechanisms are proposed for the AHE [20], in which the ${\sigma_{xy}}^A \propto \sigma_{xx}$ ($\varphi \sim 1$) in region I indicates the extrinsic skew-scattering mechanism is dominant based on the asymmetric impurity scattering caused by the spin–orbit interaction (SOI), while $\varphi \sim 0$ with a large value of ${\sigma_{xy}}^A$ in region II suggests the intrinsic Berry-phase contribution governs the AHE [23]. Recently, Onoda *et al* (2008) have developed a unified theory of the AHE in ferromagnets and proposed three scaling regions as a function of the carrier lifetime τ related Born scattering amplitude $\hbar/\tau$ ($\hbar$: Planck constant). For $\hbar/\tau < \sim E_{SO}$ (E_{SO}: spin–orbit interaction energy), $\varphi = 1$, the extrinsic skew-scattering arising from the vertex correction yields a dominant contribution; For $\sim E_{SO} < \hbar/\tau < E_F$, $\varphi = 0$, ${\sigma_{xy}}^A$ becomes insensitive to the scattering strength because of the intrinsic dissipationless topological Berry-phase contribution. Further increasing $\hbar/\tau$, $\varphi = 1.6$ [23, 24]. Usually, it is difficult to observe all the proposed regions in one ferromagnetic sample, possible due to a small variation of $\hbar/\tau$ [20, 25]. The scaling behavior in a $Sr_4Ru_3O_{10}$ flake can present all the three scaling regions indicates there is a large change of $\hbar/\tau$ in this material. The reason for such change is possibly attributed to the large variation of the structures in $Sr_4Ru_3O_{10}$ as well [14], for the two crossovers, one at about 23 K and the other at about 55 K, among the three scaling regions match well with the temperatures T_1 and T_2 shown in figure 4(a). In other words, the AHE reflects the FM nature of the flake below T_c, and which is independent on the thickness.

Figure 5 shows the saturation field H_s along the c-axis of the two flakes determined from the ρ_{xy}-H curves (see figure 3), where the inset representatively displays an enlarged ρ_{xy}-H curve of the 260 nm-thick flake measured at 40 K, and the H_s is 0.65 T indicated by the arrow. The H_s increases as the decrease of thickness at a fixed temperature, indicating that the magnetic moments in the thinner flake are more difficult to be polarized along the c-axis. In other words, the shape anisotropy caused by the decrease of thickness favors the magnetic moments aligned in the ab-plane (possibly arranged to be a weak FM order). This assignment is consistent with the observation of the metamagnetic transition ${T_m}^{flake}$ decreases with the decrease of thickness (see figure 2), where the in-plane magnetic order stabilized by the reduced thickness will suppress the metamagnetic phase.

4. Conclusions

In summary, we have investigated the transport property of two mechanically exfoliated $Sr_4Ru_3O_{10}$ nanoflakes. The result shows that the change of thickness has little effect on the FM phase, the OHE and AHE, but can modulate the metamagnetic transition temperature ${T_m}^{flake}$ significantly, which is about 25 K for the 31 nm-thick flake and 37 K for the 260 nm-thick flake, respectively. The identical Hall effect in the two flakes suggests the decrease of ${T_m}^{flake}$ cannot be attributed to the changes of the unit cell or the electronic structure. However,

we have found that the saturation field along the *c*-axis in the two flakes increases as the decrease of thickness, indicating the Ru moment is aligned closer to the *ab*-plane in the thinner flake due to the size effect, and the metamagnetic transition in $Sr_4Ru_3O_{10}$ is thus caused by a rearrangement of the Ru moments.

Acknowledgments

This work was supported by the National Natural Science Foundation of China (Grant No. 11174294, 11174291, 11374302, 11304319, U1332209, U1332139, U1432251 and U1532153), and the program of Users with Excellence, the Hefei Science Center of CAS and the CAS/SAFEA international partnership program for creative research teams of China.

References

[1] Mackenzie A P and Maeno Y 2003 The superconductivity of Sr_2RuO_4 and the physics of spin-triplet pairing *Rev. Mod. Phys.* **75** 657
[2] Grigera S A *et al* 2001 Magnetic field-tuned quantum criticality in the metallic ruthenate $Sr_3Ru_2O_7$ *Science* **294** 329–32
[3] Borzi R *et al* 2007 Formation of a nematic fluid at high fields in $Sr_3Ru_2O_7$ *Science* **315** 214–7
[4] Lester C *et al* 2015 Field-tunable spin-density-wave phases in $Sr_3Ru_2O_7$ *Nat. Mater.* **14** 373–8
[5] Klein L *et al* 1996 Anomalous spin scattering effects in the badly metallic itinerant ferromagnet $SrRuO_3$ *Phys. Rev. Lett.* **77** 2774
[6] Koster G *et al* 2012 Structure, physical properties, and applications of $SrRuO_3$ thin films *Rev. Mod. Phys.* **84** 253
[7] Crawford M *et al* 2002 Structure and magnetism of single crystal $Sr_4Ru_3O_{10}$: a ferromagnetic triple-layer ruthenate *Phys. Rev.* B **65** 214412
[8] Cao G *et al* 2003 Competing ground states in triple-layered $Sr_4Ru_3O_{10}$: verging on itinerant ferromagnetism with critical fluctuations *Phy. Rev.* B **68** 174409
[9] Gupta R *et al* 2006 Field- and pressure-induced phases in $Sr_4Ru_3O_{10}$: a spectroscopic investigation *Phys. Rev. Lett.* **96** 067004
[10] Mao Z Q *et al* 2006 Phase separation in the itinerant metamagnetic transition of $Sr_4Ru_3O_{10}$ *Phys. Rev. Lett.* **96** 077205
[11] Fobes D *et al* 2007 Phase diagram of the electronic states of trilayered ruthenate $Sr_4Ru_3O_{10}$ *Phys. Rev.* B **75** 094429
[12] Jo Y J *et al* 2007 Orbital-dependent metamagnetic response in $Sr_4Ru_3O_{10}$ *Phys. Rev.* B **75** 094413
[13] Fobes D *et al* 2010 Anisotropy of magnetoresistivities in $Sr_4Ru_3O_{10}$: evidence for an orbital-selective metamagnetic transition *Phys. Rev.* B **81** 172402
[14] Granata V *et al* 2013 Neutron diffraction study of triple-layered $Sr_4Ru_3O_{10}$ *J. Phys.: Condens. Matter.* **25** 056004
[15] Carleschi E *et al* 2014 Double metamagnetic transition in $Sr_4Ru_3O_{10}$ *Phys. Rev.* B **90** 205120
[16] Cao G *et al* 2007 Anomalous itinerant magnetism in single-crystal $Sr_4Ru_3O_{10}$: a thermodynamic and transport investigation *Phys. Rev.* B **75** 024429
[17] Xu Z *et al* 2007 Magnetic, electrical transport, and thermoelectric properties of $Sr_4Ru_3O_{10}$: evidence for a field-induced electronic phase transition at low temperatures *Phys. Rev.* B **76** 094405
[18] Mirri C *et al* 2012 Anisotropic optical conductivity of $Sr_4Ru_3O_{10}$ *Phys. Rev.* B **85** 235124
[19] Mishra S G 1990 Weak itinerant electron ferromagnets *Mod. Phys. Lett.* B **4** 83–93
[20] Nagaosa N *et al* 2010 Anomalous Hall effect *Rev. Mod. Phys.* **82** 1539
[21] Ong N P 1991 Geometric interpretation of the weak-field Hall conductivity in two-dimensional metals with arbitrary Fermi surface *Phys. Rev.* B **43** 193
[22] Mackenzie A P *et al* 1996 Hall effect in the two-dimensional metal Sr_2RuO_4 *Phys. Rev.* B **54** 7425
[23] Onoda S, Sugimoto N and Nagaosa N 2006 Intrinsic versus extrinsic anomalous hall effect in ferromagnets *Phys. Rev. Lett.* **97** 126602
[24] Onoda S, Sugimoto N and Nagaosa N 2008 Quantum transport theory of anomalous electric, thermoelectric, and thermal Hall effects in ferromagnets *Phys. Rev.* B **77** 165103
[25] Sangiao S *et al* 2009 Anomalous Hall effect in Fe (001) epitaxial thin films over a wide range in conductivity *Phys. Rev.* B **79** 014431